Electronic Supplementary Information

High-efficiency decontamination of pharmaceutical wastewater from γ-In_2Se_3/MoS_2/graphene composite driven by broad-spectrum absorption spanning ultraviolet to near-infrared irradiation

Xinyang Li[a,1], Zhigang Ruan[a,1], Ruimin Zhang[a], Junchuan Wang[a,b]*, Huayan Si[a,b]*

[a]School of Materials Science and Engineering, Shijiazhuang Tiedao University, Shijiazhuang 050043, China

[b]Hebei Provincial Key Laboratory of Traffic Engineering materials, Shijiazhuang Tiedao University, Shijiazhuang 050043, China

*Corresponding author Tel.: +86 311 8793 5411

E-mail address: sihuayan@stdu.edu.cn (H.Y. Si); wangjunchuan@stdu.edu.cn (J. C. Wang)

1 X.Y. and Z.G. contributed equally to this work.

1 Experimental section

1.1. Chemicals

Thiourea, propionic acid, Nafion, N,N-dimethylformamide, oleic acid, triethylene glycol, anhydrous sodium sulfate, N-methylpyrrolidone, sodium molybdate dihydrate, indium chloride, and selenium powder were purchased from Shanghai Aladdin Biochemical Technology Co., Ltd. All reagents are analytical purity without further purification.

1.2 Preparation of γ-In_2Se_3 nanosheets

An array of analytical-grade reagents was employed directly as received without additional purification. The γ-In_2Se_3 synthesis protocol was conducted under controlled conditions in a 100 mL three-necked round-bottom flask equipped with a condenser and maintained under an inert argon atmosphere. Following the pre-weighing of all precursor materials, the procedure proceeded as follows: (i) 0.45 mmol of selenium (Se), 0.3 mmol of indium chloride hexahydrate ($InCl_3 \cdot 4H_2O$), and 0.5 g of polyvinyl pyrrolidone (PVP) were sequentially introduced into the flask; (ii) the resulting mixture was stirred magnetically at room temperature to ensure complete dissolution; (iii) 0.1 mL of hydrazine hydrate ($N_2H_4 \cdot H_2O$) was carefully added dropwise to the solution; and (iv) the reaction mixture underwent rapid heating to 250 °C, where it was maintained for a dwell time of 30 minutes. Upon completion of the reaction, the three-necked flask was permitted to cool rapidly to ambient temperature. The synthesized product, now in its crude form, was isolated via centrifugation and subsequently purified by sequential washing with anhydrous ethanol and deionized water. Finally, the obtained material was dried under vacuum at 60 °C for complete removal of residual solvent.

1.3 Synthesis of MoS_2 nanosheets

The synthesis of MoS_2 monomers was carried out via a hydrothermal procedure, employing well-defined precursor materials and optimized reaction conditions. Sodium molybdate dihydrate ($Na_2MoO_4 \cdot 2H_2O$) (48 mg) and thiourea ($(NH_2)_2CS$) (76 mg) were

previously calcined and weighed with high precision to maintain a molar ratio of 1:5. These precursors were dissolved in 35 mL of deionized water, ensuring complete solubilization through thorough blending and magnetic stirring for 30 minutes. 10 mL of propionic acid was carefully incorporated into the solution to regulate the reaction pH. The resulting homogeneous mixture was then transferred into a 50 mL Teflon-lined stainless-steel autoclave, which was subjected to hydrothermal processing at 200 °C for an extended duration (24 h) in a convection oven. Upon completion of the reaction, the system was allowed to cool down naturally to room temperature. The black precipitate obtained post-reaction was isolated via centrifugation at 8,000 rpm for 10 minutes. The recovered product was subjected to sequential purification by washing with deionized water and ethanol to eliminate residual impurities. Finally, the purified material was dried under vacuum conditions at 60 °C for a period of 12 hours to ensure complete removal of any remaining solvent residues.

1.4 Preparation of graphene samples

Graphene was firstly exfoliated from graphite by transition metal catalysts coordinated with electrochemistry Method [1]. Then, 0.05 $g \cdot L^{-1}$ of graphene was obtained in the ethanol medium under ultrasonic dispersion treatment.

1.5 Preparation of γ-In_2Se_3/MoS_2/graphene composites

The pre-synthesized γ-In_2Se_3 nanosheets and MoS_2 nanosheets were initially mixed with triethylene glycol (TEG) solvent under ultrasonic treatment. Subsequently, reduced graphene oxide (graphene) sheets were incorporated into the suspension system. The resultant mixture underwent prolonged sonication at a power of 100 W and temperature of 30 °C for 30 minutes to ensure adequate dispersion and interfacial interaction. Following this step, the mixture was thoroughly purified by washing with ethanol and subjected to centrifugation at 8,000 rpm for two consecutive cycles, thereby yielding the γ-In_2Se_3/MoS_2/graphene composites. A critical aspect of this procedure is that the graphene content in the final composite corresponds directly to its initial amount in the precursor solution. Therefore, the exact proportion of graphene can be

accurately determined and quantified. To conduct a systematic investigation, several composite samples with varying graphene contents (1%, 2%, 3%, 4%, and 5%) were prepared under identical reaction conditions. These samples were systematically designated as γ-In_2Se_3/MoS_2/graphene-w%, where w represents the respective weight percentages (w = 1, 2, 3, 4, 5). Furthermore, for comparative purposes, a γ-In_2Se_3/MoS_2 homojunction was fabricated using an analogous synthetic process without the addition of graphene.

1.6 Characterization

The X-ray diffraction (XRD) patterns of the samples were obtained using a Bruker D8 Advance diffractometer with a source of CuKa radiation (0.15406 nm). The diffraction angle (2θ) was from 0° to 80°. The UV-Vis absorption spectra were recorded employing UV-Vis Spectrophotometer, The UV-Vis diffuse reflectance spectra of the samples were recorded on a UV4100 spectrometer (Shimadzu Company) using barium sulfate as the standard. Binding energy was determined by X-ray photoelectron spectroscopy (XPS) (Axis Supra) with Mg Ka radiation. The XPS peak was calibrated with a C 1s peak from a surface contaminating hydrocarbon with a binding energy of 284.8 eV. A Nicolet 4700 spectrometer was employed for the Fourier transform infrared (FT-IR) spectra. Transmission electron microscopy (TEM) (JEM-2100F) and energy dispersive spectrometer (EDS) were used to observe the surface of the samples before and after the photocatalytic process.

1.7 Photoelectrochemical Tests

A CHI 660B electrochemical workstation (Shanghai, China) was used to measure the photoelectrochemical properties. The working electrode is ITO glass coated by sample suspension, Pt sheet as counter electrode and Ag/AgCl electrode as reference. The electrolyte solution for the transient photocurrent test was a 0.5 M Na_2SO_4 solution. The tests were performed under the irradiation of a 300 W xenon lamp, where the light was switched on/off for a period of 10 s. The electrochemical impedance spectra (EIS) had a frequency range of 0.05 Hz-100 Hz and an amplitude of 10 mV.

1.8 Photocatalytic experiments

Tetracycline (TC) was chosen as a model pollutant to evaluate the catalytic performance of the γ-In_2Se_3/MoS_2/graphene composites. 0.5 g photocatalyst was added into 500 mL TC solution (50 mg•L^{-1}). The suspension was stirred for 60 min in the dark to reach a stable adsorption–desorption equilibrium. In order to avoid the influence of environmental warming caused by continuous light on the experimental results, the double-layer beaker was fitted with a rubber tube and connected with tap water in the order of water inlet at the bottom and water outlet at the top. Then the degradation experiment was carried out under an incandescent lamp with a power of 100 W, and 3 mL of the sample solution was taken at intervals, and 0.45 μm of the filter membrane was used to obtain the dull catalyst solution. Ultraviolet spectrophotometer was used to measure the absorption intensity of the degradation solution at different times, and the corresponding degradation efficiency was calculated by the following formula:

$$w = \frac{c_0 - c_t}{c_0} = \frac{A_0 - A_t}{A_0}$$

Where c_0 and A_0 are the initial concentration of the TCH and the corresponding absorbance value; c_t and A_t are the TCH concentration and the corresponding absorbance value when the reaction time is t.

To study the degradation mechanism of TC in the γ-In_2Se_3/MoS_2/graphene composites, electron paramagnetic resonance (EPR, EMXNANO, Bruker, Germany) spectroscopy was employed to detect the ROS captured by DMPO or TEMP. Different scavengers such as ethylenediaminetetraacetic acid (EDTA), benzoquinone (BQ), and isopropanol (IPA), were used as the scavengers of hydroxyl (·OH), holes (h^+), and superoxide ($\cdot O_2$), respectively [2]. Specifically, five 50 mL beakers were prepared and labeled as blank control, no scavenger, EDTA, IPA, and BQ, respectively. To each beaker, 20 mL of tetracycline solution was added, and the pH was adjusted to approximately 7 using 0.1 M HCl. Subsequently, 0.02 g of the ternary composite catalyst (equivalent to a concentration of 1 g/L) was added to the no scavenger, EDTA,

IPA, and BQ groups. Then, 0.2 mL of 0.1 mol/L EDTA, 0.2 mL of 1 mol/L IPA, and 0.2 mL of 0.01 mol/L BQ were introduced into the corresponding beakers. An equivalent volume of deionized water was added to both the blank control and no scavenger groups.

All beakers were stirred in the dark for 30 minutes to achieve adsorption–desorption equilibrium. Thereafter, the reaction was initiated by switching on a xenon lamp under magnetic stirring at 500 rpm. Aliquots were collected at 0, 20, 40, 60, 80, and100 minutes. Each sample was centrifuged at 8000 rpm for 10 minutes to obtain the supernatant. The absorbance of the supernatant was measured using a UV–visible spectrophotometer, and the tetracycline concentration was determined based on a pre-established calibration curve.

The studies of the degradation pathway of TC were conducted using high performance liquid chromatograph-mass spectrometry (HPLC-MS) (HPLC-Agilent Technologies 1290 Infinity, Palo Alto, CA, USA; MS-AB SCIEX QTR AP4500, Waltham, Ma, AB, USA), ZORBAX Eclipse Plus C18 Column (150 mm × 2.1 mm, 3.5 μm particle size) (Agilent, Santa Clara, CA, USA Company) and a UV detector set at 357 nm. During the process, formic acid water: acetonitrile: methanol (45:35:20) was used as the mobile phase. The flow rate was 0.2 mL/min. The mass spectra with a scan range m/z 50–500 were recorded.

2 Supplementary Figures

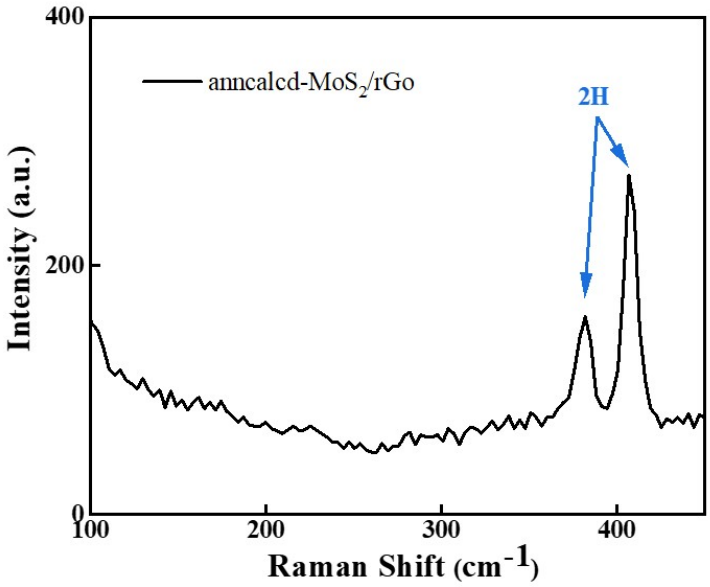

Fig. S1 Raman spectra of MoS_2.

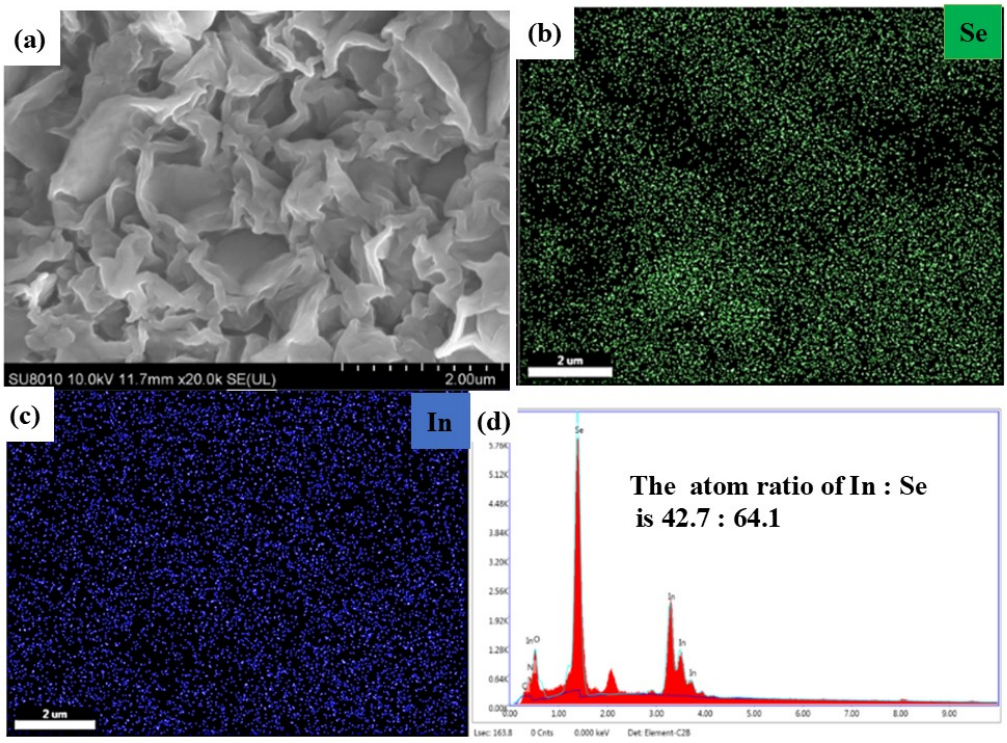

Fig. S2 EDS elemental mapping of γ-In_2Se_3.

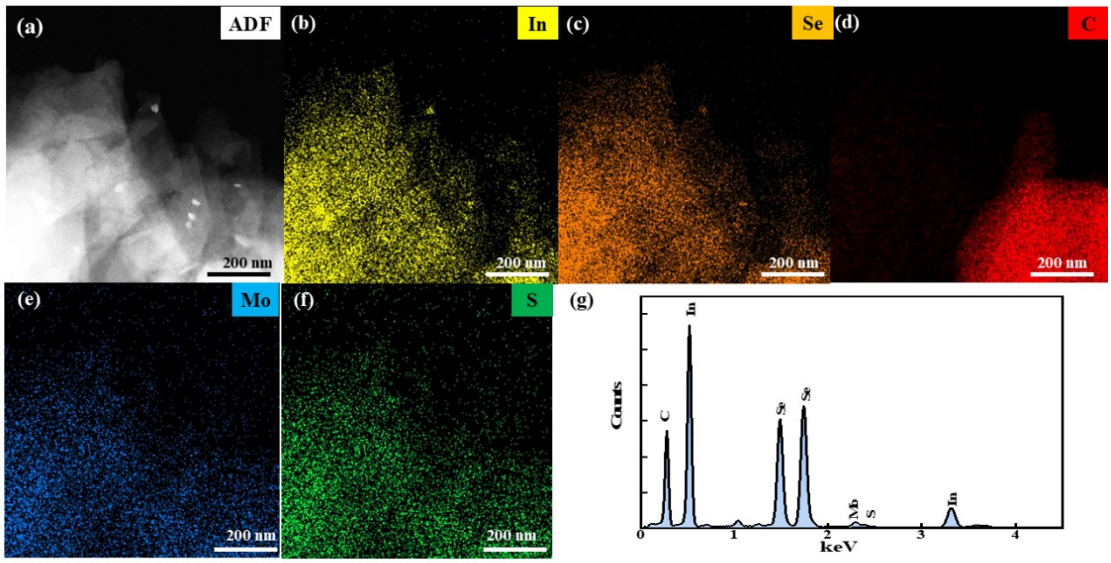

Fig. S3 EDS elemental mapping of γ-In_2Se_3/MoS_2/graphene composites.

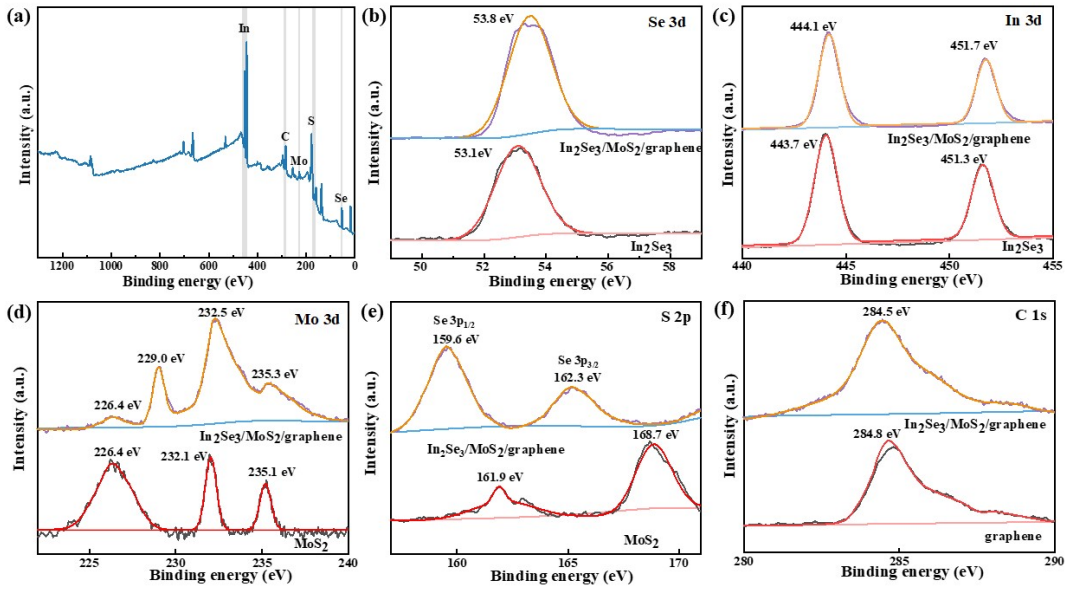

Fig. S4 High-resolution XPS spectra of γ-In_2Se_3/MoS_2/graphene composite: (a) Survey spectrum, (b) Se 3d, (c) In 3d, (d) Mo 3d, (e) S 2p and (f) C 1s. Related XPS results of γ-In_2Se_3, MoS_2 and graphene are used as references.

Table S1 A comparative summary for photocatalysis systems in TC degradation

Catalysts	TC degradation（%）	TC concentration（mg/L)	References
γ-In_2Se_3/MoS_2/graphene	91	20	this work
CW/4Co/2BNQDs	94.8	10	[3]
CuO@C	100	30	[4]
FONC@PAC	86.9	150	[5]
$Ni(OH)_2$-decorated rutile TiO_2	76	100	[6]
Fe_3O_4/g-C_3N_4/TiO_2	73.6	5	[7]
Tetragonal Prismatic γ-In_2Se_3 Nanostructures	91.5	20	[8]
$FeNi_3$/SiO_2/CuS	100	5	[9]
IL/GO/88A	95.7	10	[10]
CeO_2@UiO-66	98	20	[11]

The chemical composition and oxidation states of the γ-In_2Se_3/MoS_2/graphene composite were systematically analyzed using XPS spectroscopy. As shown in Fig. S4a, the XPS spectrum reveals distinct peaks corresponding to In, Se, Mo, S, and C elements, confirming the successful integration of these components into the composite structure. For the In 3d and Se 3d spectra (Fig. S4b and 4c), a systematic shift toward higher binding energies was observed in the composite compared to pristine γ-In_2Se_3. Specifically, the In 3d peak shifted by approximately 0.7 eV, while the Se 3d peak exhibited a slight shift of about 0.4 eV (about 0.6 eV). These shifts can be attributed to the incorporation of sulfur atoms into the structure, which possess higher electronegativity than the other components in γ-In_2Se_3. This sulfur-induced electron redistribution leads to an increased electrostatic attraction between the outer-shell electrons and the nuclei of In and Se, resulting in their stronger binding [12]. The Mo 3d XPS spectrum (Fig. S4d) exhibited an additional peak near 229 eV, which can be attributed to the Se 3s contribution. This observation aligns with known XPS data [13],

demonstrating the interplay between different elements within the composite framework. In Fig. S4e, the Se $3p_{1/2}$ and Se $3p_{3/2}$ peaks (at binding energies of 162.3 eV and 159.6 eV, respectively) dominate the XPS spectrum of the γ-In_2Se_3/MoS_2/graphene composite, effectively obscuring the S 2p peaks. This indicates a preferential oxidation state for selenium in this structural arrangement [32]. Finally, as shown in Fig. S4f, the C 1s XPS spectrum of the graphene component reveals an increased intensity of the C=C bond. Furthermore, a slight redshift in binding energy is observed, consistent with enhanced chemical interactions at the interface between γ-In_2Se_3, MoS_2, and graphene.

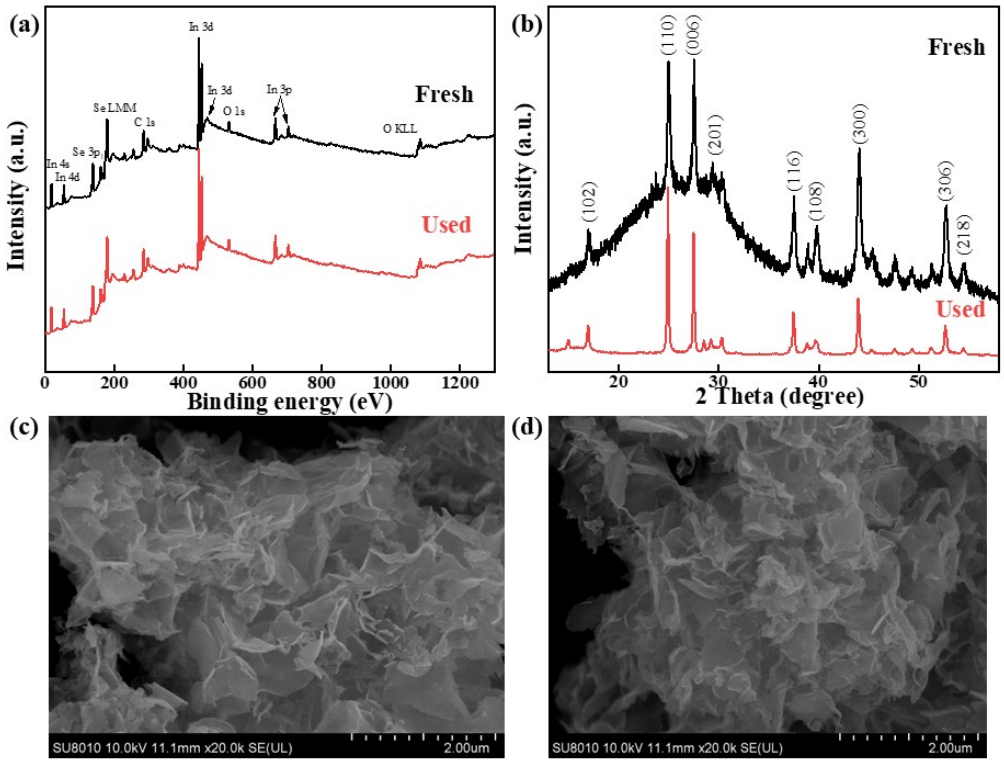

Fig. S5 (a) XPS, (b) XRD, and (c, d) SEM analyses of the composite before and after four reaction runs.

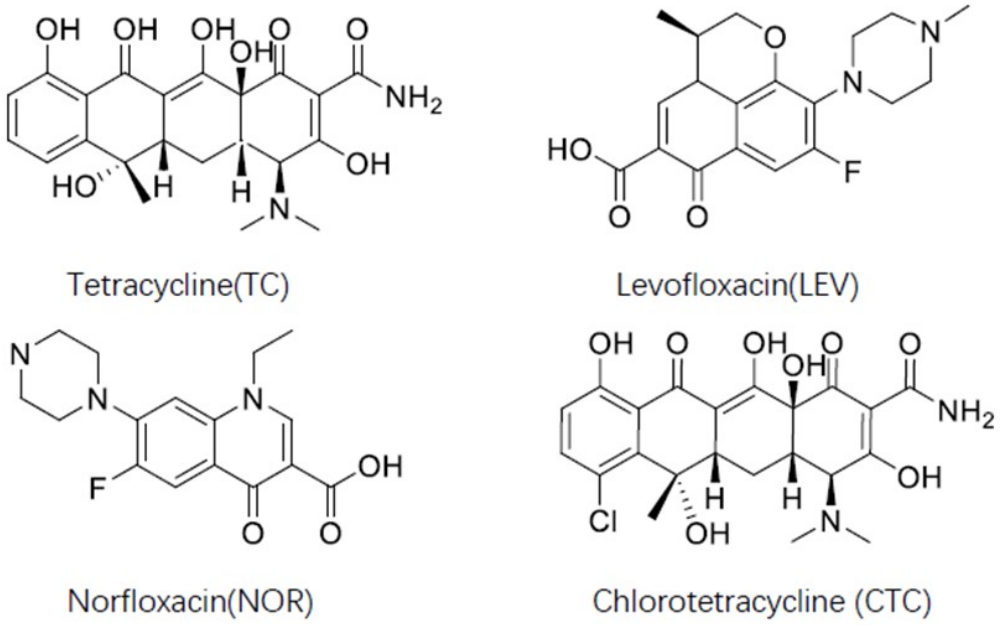

Fig. S6 Structures of the selected antibiotic pollutants.

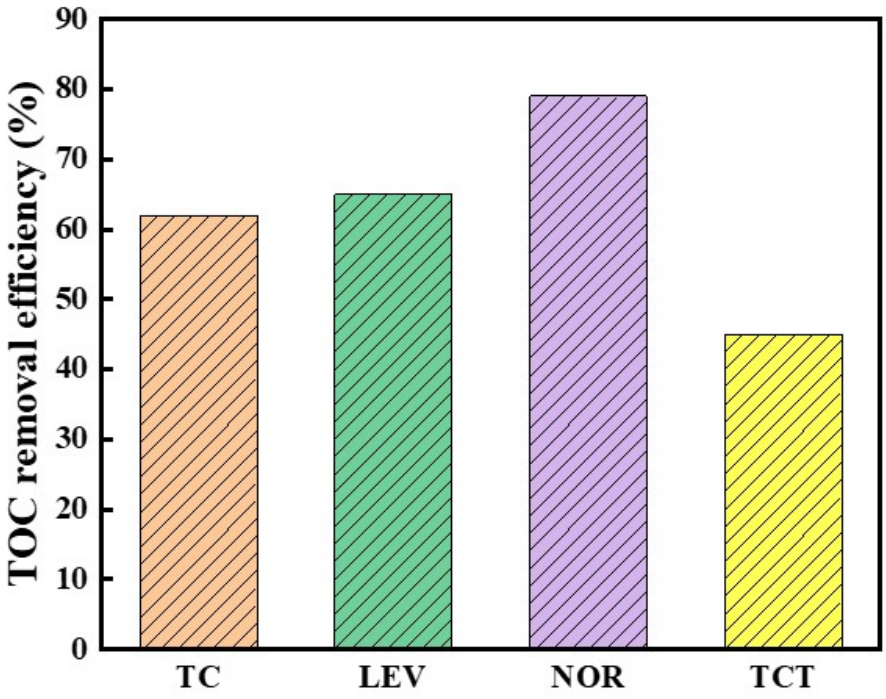

Fig. S7 Total organic carbon removal during the photodegradation process.

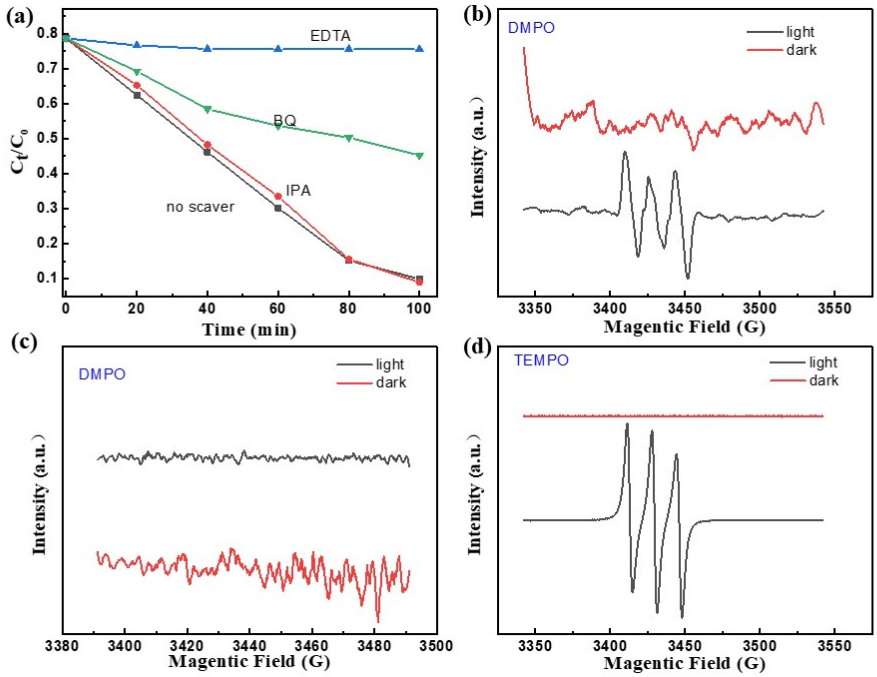

Fig. S8 (a) Effect of quenching reagents on TC degradation; (b) DMPO-·O_2^- and DMPO-·OH with irradiation for 30 s in methanol and aqueous dispersion, respectively. TEMPO-h^+ with irradiation for 30 s in methanol and aqueous dispersion.

As shown in Fig. S8a, the effects of different radical species were evaluated using specific scavenger agents. EDTA was used to capture h^+ ions; upon its addition, the photocatalytic degradation efficiency of the composite system was significantly reduced, indicating that h^+ plays a critical role in the degradation process of TC solutions. Benzyl quinoline (BQ) was employed as a scavenger for $\cdot O_2^-$ radicals, and its presence exhibited some inhibitory effects on the photocatalytic degradation efficiency. However, isopropyl alcohol (IPA), used to scavenge ·OH radicals, showed no significant impact on the photocatalytic performance of the composite system, suggesting that ·OH radicals are not dominant species in this mechanism. Based on these results, H^+ and $\cdot O_2^-$ were identified as the primary active species involved in the photocatalytic degradation of TC by the γ-In_2Se_3/MoS_2/graphene system. This conclusion was further supported by electron paramagnetic resonance (EPR) studies, which provided additional evidence for the involvement of these radicals. The EPR experiments were performed separately in methanol and water media under visible light

irradiation. As demonstrated in Fig. S8b, the presence of characteristic DMPO-·O_2^- adduct peaks confirms the involvement of ·O_2^- radicals during the photocatalytic process. In contrast, no DMPO-·OH signals were observed in Fig. S8c, indicating that ·OH radicals play a negligible role in this system. Furthermore, TEMPO-h^+ spectra in Fig. S8d revealed the distinct triplet signal characteristic of h^+ species, confirming their presence in the γ-In_2Se_3/MoS_2/graphene composite system. These observations confirm that the dominant active species responsible for TC degradation are h^+ and ·O_2^- radicals under visible light irradiation.

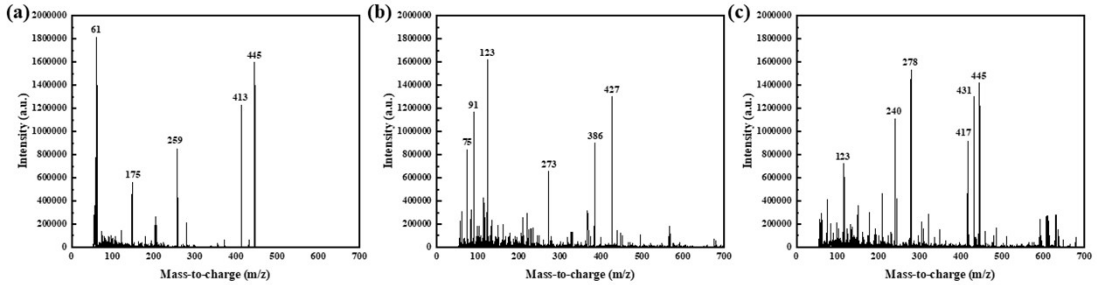

Fig. S9 The mass spectrometry of the possible intermediates of antibiotic contaminant.

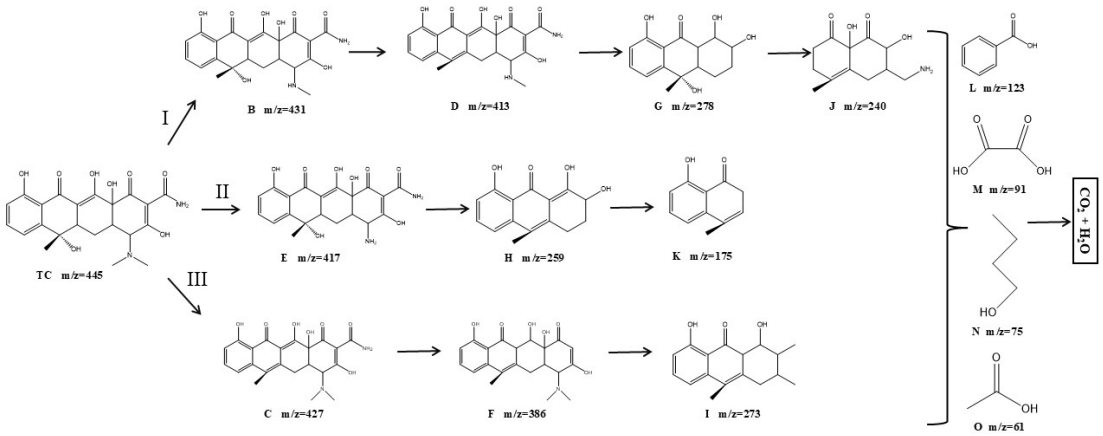

Fig. S10 Proposed TC degradation pathway in the γ-In_2Se_3/MoS_2/graphene composite system

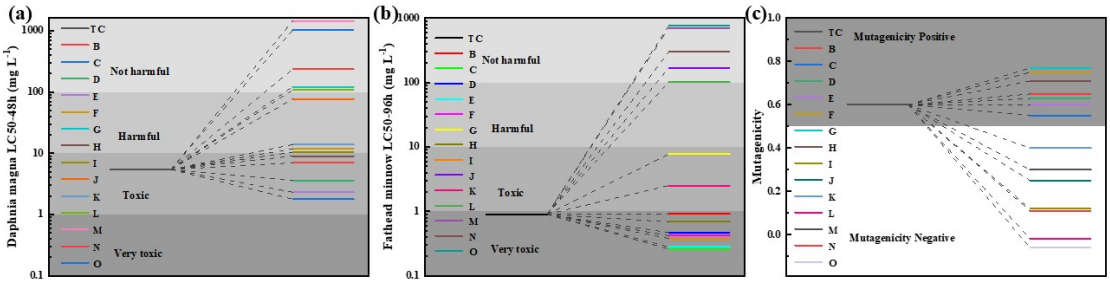

Fig. S11 (a) Daphnia magna LC50-48h of TC and degradation intermediates; (b) Fathead minnow LC50-96h of TC and degradation intermediates; (c) Mutagenicity of TC and degradation intermediates.

References

[1] H.X. Kang, K.X. Zhang, X.Y. Tian, Z.G. Ruan, Z.X. Xiao, Y.X. Jin, H.Y. Si, Y.T. Li, Transition metal catalysts coordinated with electrochemistry for preparation of graphene, Applied Catalysis O: Open, 194 (2024) 206978.

[2] W.Q. Li, L. Jin, F. Gao, H.Q. Wan, Y. Pu, X.Q. Wei, C. Chen, W.X. Zou, C.Z. Zhu, L. Dong, Advantageous roles of phosphate decorated octahedral CeO_2 {111}/g-C_3N_4 in boosting photocatalytic CO_2 reduction: Charge transfer bridge and Lewis basic site, Applied Catalysis B: Environmental, 294 (2021) 120257.

[3] R. Chen, H. Zhang, Y. Dong, H. Shi, Dual metal ions/BNQDs boost PMS activation over copper tungstate photocatalyst for antibiotic removal: Intermediate, toxicity assessment and mechanism, Journal of Materials Science & Technology, 170 (2023) 11-24.

[4] D. Yang, P. Hong, Y. Hu, Y. Li, C. Wang, J. He, B. Sun, S. Zhu, L. Kong, J. Liu, Carbon framework-encapsulated copper oxide particles to activate peroxymonosulfate for the efficient degradation of tetracycline, Applied Surface Science, 552 (2021) 149424.

[5] J.H. Zhou, X.S. Li, J. Yuan, Z.W. Wang, Efficient degradation and toxicity reduction of tetracycline by recyclable ferroferric oxide doped powdered activated charcoal via peroxymonosulfate (PMS) activation, Chemical Engineering Journal, 441 (2022) 136061.

[6] S. Leong, D. Li, K. Hapgood, X. Zhang, H. Wang, $Ni(OH)_2$ decorated rutile TiO_2 for efficient removal of tetracycline from wastewater, Applied Catalysis B: Environmental, 198 (2016) 224-233.

[7] R. Liu, X. Zhang, X. Han, Y. Sun, S. Jin, R.J. Liu, Photocatalytic degradation of tetracycline with Fe_3O_4/g-C_3N_4/TiO_2 catalyst under visible light, Carbon Letters, 34 (2024) 75 - 83.

[8] X.F. Wei, H. Feng, L.W. Li, J.B. Gong, K. Jiang, S.L. Xue, P.K. Chu, Synthesis of Tetragonal Prismatic r-In2Se3 Nanostructures with Predominantly {110} Facets and Photocatalytic Degradation of Tetracycline, Applied Catalysis B: Environmental, 260 (2020) 18218.

[9] N. Nasseh, B. Barikbin, L. Taghavi, Photocatalytic degradation of tetracycline hydrochloride by $FeNi_3$/SiO_2/CuS magnetic nanocomposite under simulated solar irradiation: Efficiency, stability, kinetic and pathway study, Environmental Technology & Innovation, 20 (2020) 101035.

[10] H.Y. Chen, H. Tao, D.M. Li, J.H. Cheng, K. Du, Synthesis of IL/GO/88A and its photocatalytic degradation performance for tetracycline, Chinese Journal of Environmental Engineering, 15 (2021) 1862-1872.

[11] L. Zhang, X.J. Gong, L.H. Li, Photocatalytic degradation of tetracycline hydrochloride by CeO_2@UiO-66, Journal of Liaoning Petrochemical University, 44 (2024) 8-14.

[12] J. Y., W. Q., H. L., Z.X. Y., L.F. Y., Construction of In_2Se_3/MoS_2 heterojunction as photoanode toward efficient photoelectrochemical water splitting, Chem. Eng. J., 358 (2019) 752–758.

[13] D.W. Langer, C.J. Vesely, Electronic core levels of zinc chalcogenides, Phys. Rev. B, 2 (1970) 4885.